NMR characterization of PAMAM–G5.NH2 entrapped atomic and molecular assemblies

4 AUTHORS:

Mónika Kéri
University of Debrecen
5 PUBLICATIONS   **20** CITATIONS

SEE PROFILE

Chen Peng
Donghua University
30 PUBLICATIONS   **926** CITATIONS

SEE PROFILE

Xiangyang Shi
Donghua University
219 PUBLICATIONS   **7,061** CITATIONS

SEE PROFILE

Istvan Banyai
University of Debrecen
64 PUBLICATIONS   **987** CITATIONS

SEE PROFILE

NMR Characterization of PAMAM_G5.NH₂ Entrapped Atomic and Molecular Assemblies

Mónika Kéri,[†] Chen Peng,[‡] Xiangyang Shi,[‡,§] and István Bányai*[,†]

[†]Department of Colloid and Environmental Chemistry, University of Debrecen, Debrecen, Hungary
[‡]State Key Laboratory for Modification of Chemical Fibers and Polymer Materials, College of Materials Science and Engineering and
[§]College of Chemistry, Chemical Engineering and Biotechnology, Donghua University, Shanghai 201620, People's Republic of China

S *Supporting Information*

ABSTRACT: High resolution NMR spectroscopy, NMR diffusiometry, and NMR cryoporometry have been used to investigate aqueous solution (D_2O) of $PAMAM\_G5.NH_2$-$(Au)_{25-100}$ and $PAMAM\_G5.NH_2$-$(H_2O)_{1000}$-$(H_2O)_{4000}$ systems. In the case of dendrimer entrapped gold nanoparticles, the detailed analysis of high resolution NMR spectra has shown that no precursor complex formation happens under the circumstances applied for reduction. Further PGSE results verify that gold nanoparticles of 1.9−2.6 nm size are entrapped in the outermost part of the dendrimers and probably more than one dendrimer molecule takes part in the stabilization process. This system looks like a transition state between dendrimer encapsulated nanoparticles (DENs) and dendrimer stabilized nanoparticles (DSNs),

and we deal with it in details for what this means. NMR cryoporometry experiments were performed to detect the encapsulation of water molecules. The results show that, in the swelling $PAMAM\_G5.NH_2$ dendrimers, by adding water step by step, there are specific cavities for water with diameters of 3.6 and 5.2 nm. These cavities have a penetrable wall for water molecules and probably exist very close to the terminal groups. The permeability of the cavities is increasing with the increase of the water content. In dilute solution, the formation of nanoparticles is determined by the ratio of the rate of nucleation and aggregation and the latter is affected by the $PAMAM\_G5.NH_2$.
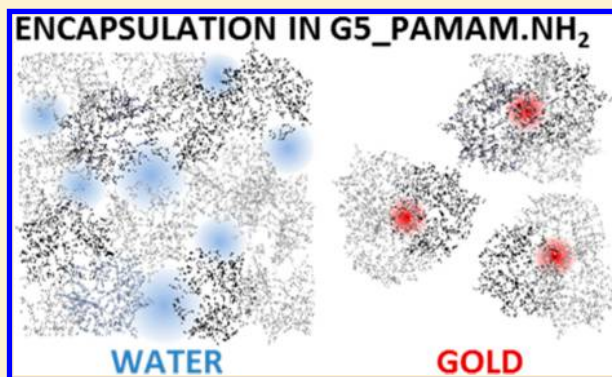
INTRODUCTION

We report here the use of different types of solution NMR spectroscopy on generation five poly(amidoamine) dendrimer ($PAMAM\_G5.NH_2$) containing gold nanoparticles and on the inclusion of water molecules into this macromolecule. TEM studies showed that at 25, 50, 75 and 100 Au(III)/$PAMAM\_G5.NH_2$ precursor ratio gold nanoparticles (AuNPs) of 1.9, 2.2, 2.5, and 2.6 nm were included in the dendrimers forming hybrid nanoparticles.[1] After redispersion of hybrid AuNPs to D_2O, PGSE NMR experiments show that there are remarkable differences in the diffusion rate between $G5\_PAMAM.NH_2$ and the gold loaded dendrimers, indicating that 3−4 dendrimer molecules encapsulate one AuNP. High resolution ^1H NMR studies show changes in chemical shifts for CH_2 protons of the terminal groups in the presence of gold nanoparticles. Taking the results presented here together, we come to a conclusion that $G5\_PAMAM.NH_2$ dendrimer behaves somehow as a transition between the steric stabilizing and encapsulating agents, as Gröhn et al. predict in their paper.[2] NMR cryoporometry experiments performed on $G5\_PA$-$MAM.NH_2$-$(H_2O)_x$ systems (x = 1000−4000) allow one to get a deeper insight into the ability of dendrimers to be a template and to encapsulate molecular assemblies. Our results show that the dendrimer loaded with water step by step swells

in the way that water droplets form in it with well-determined sizes. The wall of these filled cavities is penetrable for the water molecules, as PGSE NMR shows, and the permeability depends on water content.

PAMAM dendrimers have been used as a template for metal nanoparticles back to the discovery of these starburst polymers.[3−9] Their nature is basically different from the usual stabilizing agents because the nanoparticles are sterically confined in the interior region and therefore their activity changes only slightly.[10] Two basic types of dendrimer−gold atomic assembly systems are classified in the literature called dendrimer encapsulated (*intra*dendrimer) nanoparticles (DENs) and dendrimer stabilized (*inter*dendrimer) nanoparticles (DSNs).[11] Both types of nanoparticles are important as catalysts, contrast agents, and nanosized drug carriers. There are well documented recipes for preparation and analytical techniques for characterization of both types of dendrimer mediated nanoparticles.[2,10,11] It is widely accepted that the first step of the synthesis of metal DENs is complex formation between the metal ions and the donor groups of dendrimers. However, there are indications that for gold it is not always the

case.[2,12] The molar ratio of metal ions to dendrimer end groups is one of the main features determining whether DENs or DSNs will form.[2]

Characterization of DENs is not an easy task because of their small size and the inclusion in a large organic framework. Sometimes the differentiation between DENs and DSNs is not obvious.[10] TEM pictures are most often used, and they are even more attractive if the organic shell is stained with heavy metal salt.[2] However, there is always a doubt of whether the solidified colloids behave in the same way as in solutions. The main question addressed to *in situ* (solution) characterization is proving of the encapsulation. Indirect proof for existence of Pt-DENs was found by CO adsorption and solvent-selective poisoning Pt-DEN catalyst.[13,14] However, the most promising technique is NMR spectroscopy.[15] With high-resolution NMR, Gomez et al. presented a simple, clever method to determine the size of encapsulated PdDENs based on the increased relaxation rate of protons of G4_PAMAM.OH dendrimer attached to the encapsulated metal colloid.[16,17] Furthermore, 1D and 2D variants of NMR are useful for assignments of peaks and to detect the existence and the donor atoms of precomplex formation.[17] Also, NMR diffusiometry (PGSE or PFGSE) can be used to measure the hydrodynamic size of DENs as well as the quasi-elastic light scattering (QLS).[18] The little change in hydrodynamic radius compared to the dendrimer host is supposed to be an indication of encapsulation. The DSNs are associates and therefore have a slower diffusion rate according to the experiences.[17]

Gröhn et al. systematically studied the formation of gold colloids in the presence of G2 to G10_PAMAM.NH$_2$ dendrimers and found that if the reduction by NaBH$_4$ is slow enough then dendrimers are effective templates for the formation of well-defined hybrid nanoparticles. They introduced the hybrid definition for the assembly of gold colloids and the organic macromolecules. Their results indicated that the density of formed gold nanoparticles corresponds to the bulk density of gold and the size of DENs could be regulated by the (gold atom)/(dendrimer end group) ratio varied up to 1:1 without precipitating.[2] The effect of dendrimer generation showed that from G2 to G4 DSNs formed of larger size than expected while from G6 to G9 DENs formed with size determined by the number of gold atoms added ("fixed loading law"). The G5_PAMAM.NH$_2$ dendrimer could not be characterized precisely, while one G10_PAMAM.NH$_2$ molecule contained several smaller gold nanoparticles.[2]

Kim et al. prepared 1−2 nm small gold DENs having a very narrow size distribution using G4 and G6_PAMAM.Q$_p$ dendrimer cations as templates, where Q stands for quaternary trimethyl-ammonium end groups.[19] The dendrimers, charged up to positive in this way, did not aggregate and encapsulated as many gold atoms per molecule as many gold ions per molecule were added. These gold nanoparticles also had the same density as bulk gold. Recently, two papers reported that gold may have a different density than that of the bulk. Ackerson et al. prepared thiolate stabilized monodisperse gold nanoparticles of 2 nm size containing 144 gold atoms determined by high-angle annular dark-field scanning transmission electron microscope.[20] It corresponds to a density 1.7 times lighter than that of the bulk gold. Lu et al. also found this phenomenon by preparing gold nanoparticles of 3 nm size containing 479 gold atoms.[21] In this latter case, the number of gold atoms was determined by very accurate osmotic pressure measurements. They explained the reported observations on the different number of atoms in

nanoparticles of the same size with four factors. The first three factors connected to the obligate uncertainty and errors of analytical methods. The fourth one is that the organic part of the stabilizer is built into the gold nanoparticles, resulting in a decrease of density and as a consequence causing over-estimation of the number of gold atoms/nanoparticles.

Recently, we have reported the preparation and application of larger entrapped gold nanoparticles (1.9−2.6 nm) using G5_PAMAM.NH$_2$ dendrimers as templates.[1] In many respects of applications, they have behaved as DENs, but because of the relatively large TEM size of the obtained AuNPs, we present here a detailed *in situ* examination of these systems.[1,22−24] Gröhn et al. could not characterize whether G5_PAMAM.NH$_2$ dendrimer would stabilize gold colloid sterically or encapsulate it. It behaved as a borderline between the lower and higher generations.[2,12] However, Kim et al. could encapsulate gold even into fourth generation, G4_PAMAM.Q$_{32}$ dendrimer if it had been decorated with positive charges producing extra small DENs.[19] Also, an interesting point is the *in situ* structure of dendrimers from a stabilizing point of view. For G5_PA-MAM.X (where X is NH$_2$ or succinic acid amide, SAH), hydration numbers in dilute solution were determined by NMR diffusiometry as about 3700 depending on the model chosen.[25] The study of the swelling mechanism of G5_PAMAM.NH$_2$ by adding water step by step by NMR cryoporometry can give useful information on the possible cavities and the encapsulation capability of dendrimers. We are convinced that this detailed study of the AuNP formation combined with investigation of the presence or formation of cavities in a hydrated dendrimer itself will provide us with a deeper insight into the extraordinary templating capability of PAMAM dendrimers reported frequently.[4,5,10,11]

■ EXPERIMENTAL SECTION

Synthesis of AuNPs. AuNPs were synthesized according to a procedure described in our previous papers.[22−24] In brief, AuNPs were synthesized using sodium borohydride (Sigma-Aldrich) for reduction of AuCl$_4^-$ (Reanal, Hungary) and G5.NH$_2$ dendrimers (Dendritech) as templates with different (Au(III)-ion)/(dendrimer) molar ratios at ice-water temperature. The reaction mixture was dialyzed against 4 L of water six times for 3 days and lyophilized for storing. All other every day laboratory chemicals were purchased from Sigma-Aldrich and used without further purification. For synthesis, dilution, and dissolution, Milli-Q (18 MΩ cm) water was used.

Characterization. The formed AuNPs were characterized by UV−vis spectroscopy and transmission electron microscopy to further confirm the size change. TEM was performed with a JEOL 2010F analytical electron microscope (Tokyo, Japan) at 200 kV. Each sample was dispersed in water at a concentration of 1 mg/mL, dropped onto a carbon-coated copper grid, and air-dried before measurement. The sizes of Au DENPs were measured by using Imagepro plus software, version 6.0. To analyze the size, 300 NPs were randomly selected for each sample. The formed AuNPs with the Au atom/dendrimer molar ratio at 25:1, 50:1, 75:1, and 100:1 have an average AuNP size of 1.9, 2.2, 2.5, and 2.6 nm, respectively, as published.[1,22] G5.NH$_2$ dendrimers and the synthesized AuNPs were dissolved in water. The number of primary amines was determined by Megazyme's Primary Amino Nitrogen (PAN-OPA) Assay Kit according to the manufacturer's instruction.[1]

For NMR experiments, solid AuNPs (typically 4−6 mg/500 μL of D$_2$O (99.9 deut % Sigma-Aldrich)) were dispersed into

Table 1. Physico-Chemical Characteristics of the Prepared AuNPs and Hybrids[a]

Au/G5.NH$_2$ ratio ($n_{Au(III)}$)	aver. TEM size of AuNPs[1] (nm)	no. of free NH$_2$ groups[1]	aver. diffusion coeff., D_{meas} (m^2/s)	average hydrodynamic size[b] (nm)	no. of Au/AuNP (n_{Au})
0	n/a	123.3	6.5 × 10^{-11} [25]	6.14	n/a
25	1.9	67	5.3 × 10^{-11}	7.6	210
50	2.2	61.3	5.6 × 10^{-11}	7.1	330
75	2.5	55.3	5.3 × 10^{-11}	7.6	480
100	2.6	51.6	5.7 × 10^{-11}	7.0	541

[a]T = 298 K. [b]These size values were calculated from the averaged diffusion coefficient by the Einstein−Stokes equation and were not used in further discussions.

deuterium oxide and sonicated for 5−10 min and introduced into NMR tubes of 5 mm outer diameter. The 1D and 2D ^{1}H NMR experiments for assignment were performed by means of a Bruker DRX 400 NMR spectrometer using standard pulse programs provided with the spectrometer. TopSpin (Bruker) software was used for post processing. To characterize the interaction of PAMAM_G5.NH$_2$ with Au(III) ions, 12.2 mg of dendrimer was dissolved in 800 μL of D$_2$O, and 600 μL of AuCl$_3$ solution (10 mg/mL) was added in four steps. pH was measured, and ^{1}H NMR and diffusion ordered spectroscopy (DOSY) NMR measurements were carried out.

NMR Diffusiometry. A stimulated spin echo pulse sequence was employed using bipolar gradient pulses to decrease eddy currents (BIPLED) at 298 + 0.2 K. A Eurotherm unit was used for stabilizing or regulating the temperature with air flow through a Bruker BSCU 05 cooling unit. The diffusion coefficient of water (D$_2$O) was determined in every sample in order to check the state of the instrument. Typical parameters for diffusion experiments were diffusion times of Δ = 15 ms (water) and 50 ms (nanoparticles) and lengths of gradient pulses of δ = 4 ms (water) and 8 ms (nanoparticles). The diffusion data were evaluated according to eq 1:

$$I = I_0 \exp(-D_{obs}(\Delta - \delta/3)\gamma^2\delta^2G^2) \qquad (1)$$

The pulsed gradient strength (G) increased with 32 square distant steps from 0 to approximately 50 G cm^{-1}. $D_{obs}\gamma^2$ was calculated after fitting the exponential curve (1) on the measured echo intensity, I, as a function of G^2 (determined by the number of experiments) using the known parameters (see the Supporting Information, Figure S1). The real diffusion coefficient D was calculated as $\kappa D_{obs}\gamma^2$, where κ is the calibration constant of the gradient. The calibration of the gradient was made for D$_2$O according to our previous paper.[25] MestreNova 8.1 software was used for post processing.

NMR Cryoporometry. NMR cryoporometry in its basic form is a combination of an old discovery and a relatively new technique.[26] The method is based on the detection of the fraction of melted phase at different temperatures by liquid phase NMR and the determination of melting/freezing point depression of confined liquid in small pores. The application uses the so-called modified Gibbs−Thomson equations:

$$\Delta T_{m/f} = T_{m/f} - T_0 = -\frac{nK_c}{r_p} \qquad (2)$$

discussed and analyzed in detail by Strange et al. and Furó and Petrov.[26−28] In eq 2, $\Delta T_{m/f}$ is the melting/freezing point depression expressed as a difference between the bulk (T_0) and confined liquid ($T_{m/f}$) phase transition. K_c is the cryoporometric constant, n is a geometric factor, and r_p is the pore size. In our experiments, lyophilized dendrimer (Dendritech), 77.4 mg, was put into an NMR tube in a drybox under a nitrogen

atmosphere, and was mixed with 1000−4000 mol of water/1 mol of G5.NH$_2$ in four steps adding 1000 mol of water/ dendrimer in each step. Between each step, we waited at least 7 days for the polymer gel to form and the water to diffuse into the gel before the NMR experiments. The samples were frozen completely in a plastic NMR tube at −40 °C. The probe head temperature was also cooled to this temperature, and after temperature equilibration, the ^{1}H NMR spectrum of the sample was recorded by a spin echo sequence.[28] The typical echo time was 0.5 ms, and the length of the 90° pulse was around 5.4 μs determined in every case. By using an automatic program, the temperature was elevated up to 5 °C with 0.5 °C steps and NMR spectra were recorded. In each temperature step, the waiting time was set to 5 min which proved enough for the sample to take up the temperature (see the Supporting Information, Figure S3). The FIDs were processed by MestreNova 8.1 software, and the integrated intensities of water peak were plotted against the temperature. The temperature was calibrated on glycol and methanol.[29] The K_c for water was taken from the literature as 30 nm K.[28] We considered the formation of spherical pores in the swelling dendrimer; therefore, n = 2 was used for calculation.

RESULTS AND DISCUSSION

Characterization of Dendrimer−Gold Hybrid Nanoparticles. In Table 1, we summarize the measured and calculated physicochemical data of AuNPs and gold−dendrimer hybrid nanoparticles. The gold−dendrimer hybrid nanoparticles contained gold colloids with diameters of 1.9−2.6 nm depending on the gold atom dendrimer molecule ratio. The number of amino end groups was determined by pH potentiometric titration for PAMAM_G5.NH$_2$ in the absence of AuNPs. In the presence of AuNPs, the lack of approximately 50% of NH$_2$ end groups compared to the free dendrimer was found. It means that a certain amount of amino end groups is not accessible for reagent, as we presented in our previous paper.[1]

From high resolution NMR, we can get further evidence on the location of gold nanoparticles within G5.NH$_2$. In Figure 1, ^{1}H NMR spectra of the dissolved hybrid nanoparticles are shown, and in Scheme 1, the numbering of dendrimer protons is drawn. The ^{1}H NMR peaks of 23 and 24 CH$_2$ protons move to higher value chemical shifts, indicating the proximity of the gold surface. We can conclude that AuNPs are in the outermost part of the G5.NH$_2$ dendrimer.

From PFGSE NMR experiments, we can see that the hybrid nanoparticles have a lower average diffusion rate compared to the free dendrimer, as reported in Table 1. The question arises as to what is the meaning of this value in our system. If we suppose that the structure, therefore the density as well, of the gold nanoparticles corresponds to the bulk gold, we can
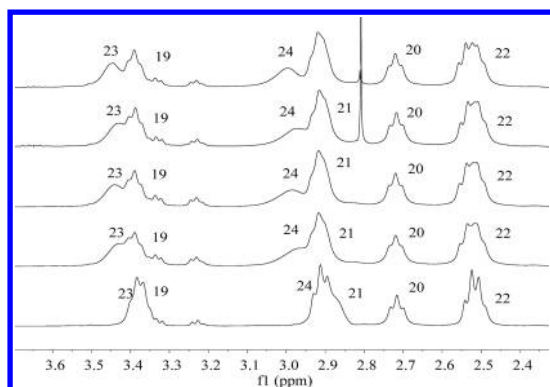
Figure 1. ^{1}H NMR spectra of dispersed D_2O solution of Au-hybrid nanoparticles. The bottom spectrum is without AuNPs. The next spectra from bottom to top are the samples prepared by addition of 25, 50, 75, and 100 Au(III) ions in the preparation and redispersed in D_2O. The numbers are explained in Scheme 1.

Scheme 1. Numbering of Protons in G5_PAMAM.NH$_2$ Dendrimer for NMR Spectra[a]
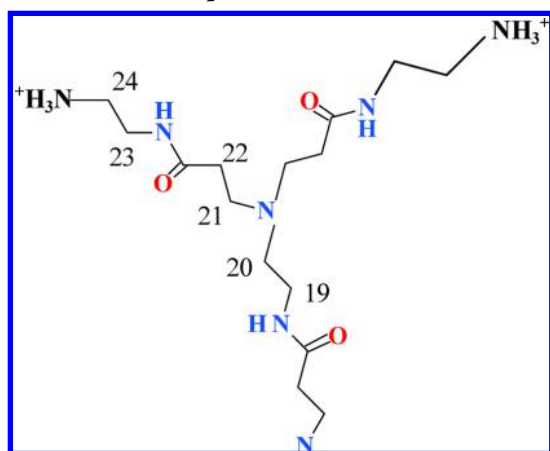
[a]One outer arm is shown. The numbers in NMR spectra (Figure 1) include the same inner side protons, i.e., 22 denotes all protons which are in the direct neighborhood of the CO group.[25]

calculate from the TEM size the average number of gold atoms in the nanoparticles of a given size. These values are shown in Table 1. It is seen that there are 6−8 times more gold atoms in one nanoparticle (n_{Au}) than expected from the added Au(III) ($n_{Au(III)}$) per mole of dendrimer. There are indications in the literature that the number of gold atoms may be lower if the structure of the nanoparticles is different from the bulk gold.[20,21] However, if we took that into consideration, it would result in still a 4−5 times larger number of gold atoms in one

nanoparticle than the number of added gold ions/molecule of dendrimer. In diffusion curves, we found only single exponential decays, and therefore, fast chemical exchange on the diffusion NMR time scale should take place between the different forms of dendrimers (see the Supporting Information, Figure S1). The NMR spectra shown in Figure 1 also indicate that only one set of peaks are present; therefore, the exchange process is also fast on the time scale of chemical shift differences. The interpretation of the averaged hydrodynamic sizes calculated from the averaged diffusion coefficients measured in the systems can be made with the following two-site model.

$$D_nG + D^* \rightleftharpoons D_{n-1}D^*G + D \qquad (3)$$

where n is the number of dendrimers (D) interacting with gold (G). In other words, more than one dendrimer interacts with one AuNP in the hybrid. This type of equilibrium has already been suggested by Garcia et al.[6] If the equilibrium is fast, then this model will lead to eq 4 for the measured diffusion coefficient (D_{meas}) as

$$D_{meas} = x_D D_D + x_{D(G)} D_{D(G)} \qquad (4)$$

where x_D and $x_{D(G)}$ stand for the molar fraction of the free and bounded dendrimers, respectively, while D_D and $D_{D(G)}$ are the diffusion coefficients accordingly. The number of dendrimers interacting with gold nanoparticles, n, is a crucial question for this model. In Table 2, we calculated the possible hydrodynamic sizes ($R_{D(G)}$) of hybrid nanoparticles supposing compositions of the assemblies from D_1G to D_5G ($n = 1$ to $n = 5$) for all Au(III) concentrations as follows. First, we substitute the Einsten−Stokes formula into eq 4

$$D_{meas} = x_D D_D + x_{D(G)} \frac{k_B T}{6\pi\eta R_{D(G)}} \qquad (5)$$

where $R_{D(G)}$ is the hydrodynamic radius of the hybrid nanoparticle while the other symbols have their usual meaning. Then, we can rewrite eq 5 as

$$R_{D(G)} = \frac{x_{D(G)} k_B T}{6\pi\eta (D_{meas} - x_D D_D)} \qquad (6)$$

In this equation, $x_{D(G)}$ can be calculated as $n \times n_{Au(III)}/n_{Au}$. For example, in the case when 25 gold ions were added to one dendrimer ($n_{Au(III)} = 25$, Table 1) and it was supposed that two dendrimers ($n = 2$) entrap one gold particle, $x_{D(G)} = (2 \times 25)/210 = 0.24$ and $x_D = 0.76$ using $n_{Au} = 210$ from Table 1. The hydrodynamic radius of the hypothetic D_2G hybrid is $R_{D(G)} = (0.24 \times 1.38 \times 10^{-23} \times 298)/(6 \times 3.14 \times 1.095 \times 10^{-3} \times (5.3 \times 10^{-11} - 0.76 \times 6.5 \times 10^{-11})) = 13.8$ nm, and the diameter is

Table 2. Ratio of Bounded Dendrimers and the Size of the Hybrid Nanoparticles at Different Au:G5.NH$_2$ and AuNP:G5.NH$_2$ Ratios

AuNP/G5.NH$_2$	25:1		50:1		75:1		100:1	
	$x_{D(G)}$	d (nm)	$x_{D(G)}$	d (nm)	$x_{D(G)}$	d (nm)	$x_{D(G)}$	d (nm)
1:1	0.12	−11.2[a]	0.15	71.7	0.16	−34.0[a]	0.18	18.5
1:2	0.24	27.5	0.30	11.4	0.31	15.1	0.37	9.3
1:3	0.36	12.8	0.45	8.9	0.47	10.2	0.55	7.9
1:4	0.48	10.1	0.61	8.0	0.63	8.8	0.74	7.4
1:5	0.60	8.95	0.76	7.56	0.78	8.09	0.92	7.12

[a]Negative diameter indicates that the 1:1 dendrimer/AuNP model is not correct.

27.5 nm. The obtained hydrodynamic radii for other D_nG at other ratios are given in Table 2.

To decide the possible number of dendrimers stabilizing the AuNPs (n), we investigated the given hypothetic sizes, based on eq 6, and compared to literature data. There are two approaches for the estimation of the diffusion coefficient (D_2) and size (R_2) of a dimeric macromolecule compared to those of the monomer (D_1 and R_1). (1) Regarding the dimer as two spheres, forming a prolate ellipsoid (axial ratio 2:1), $D_2/D_1 = 0.706$ or $R_2/R_1 = 1/0.706 = 1.42$ according to the Stokes–Einstein equation.[30] (2) Regarding the dimer as a sphere with a double volume of the monomer, $D_2/D_1 = 0.79$; therefore, $R_2/R_1 = 1.27$.[30−32] We applied these two models to estimate the lower and upper limits of the size of D_2G hybrid AuNPs. Since the radius of PAMAM_G5.NH$_2$ is 3.07 nm (Table 1), R_{D2G} may vary from 4.36 nm (model 1) to 3.9 nm (model 2). Thus, the diameter of D_2G is between 7.8 and 8.7 nm. The second model allows us to estimate the diameters for D_3G, D_4G, and D_5G, resulting in 8.8, 9.8, and 10.5 nm, respectively. Relevant experimental results are also available. Van Dongen et al. published accurate experimental hydrodynamic diameters for G5.NH$_2$ covalent oligomers from 2 to 4 between 8 and 9.2 nm.[33] Considering the models and the experiments, it seems to be obvious that diameters for D_1G, D_2G, and D_5G in Table 2 are not realistic, since the given sizes are too large for D_2G and too small for D_5G. Therefore, 1:1, 1:2, and 1:5 hybrid AuNPs can be ruled out. Thus, we can suppose that in our system D_3G or D_4G are most probably present taking into account the experimental uncertainties.

In the literature[6,10] and according to our experiences,[1,22−24] the application of G5.NH$_2$ resulted in 2–3 nm AuNPs under different conditions which behaved in many applications as encapsulated nanoparticles. However, our results prove that one G5.NH$_2$ dendrimer molecule cannot encapsulate a AuNP of this size. According to Gröhn et al., only higher generation dendrimers (G6-8.NH$_2$) entrap AuNPs of 2–3.2 nm.[2] The classical steric stabilization is not probable either because much larger AuNPs should form to ensure more dendrimers of this size adsorbing on the surface. In our explanation, AuNPs are partially encapsulated into the dendrimers, which is supported by our ^{1}H NMR results (Figure 1). G5.NH$_2$ behaves as a transition between a steric stabilizer and an encapsulating agent in this way.

Characterization of Dendrimer−Au(III) Ion Interaction. It is widely accepted that the interaction between Au(III) ions and dendrimers before reduction plays a certain role in the size and structure of AuNPs or hybrid particles formed during the synthesis.[10]

Therefore, we investigated this interaction by the evaluation of ^{1}H NMR spectra of G5.NH$_2$ in the presence of an increasing amount of Au(III) species (Supporting Information, Figure S2). Since the ^{1}H NMR spectra of G5.NH$_2$ are pH sensitive, we compared the changes at appropriate pH values. In Figure 2, the change of ^{1}H NMR chemical shifts of protons on terminal carbons 23 and 24 as a function of pH in the presence of Au(III) is shown. The chemical shifts of CH$_2$ protons of the 24 and 23 carbons show slight changes to lower ppm in the presence of Au(III). At this pH, the periphery of G5.NH$_2$ holds a large positive charge because of the protonation. The chemical shifts of the inner 19−22 CH$_2$ protons show negligible differences because in this pH range the tertiary amino groups are less protonated (see the Supporting Information, Figure S2). The chemical shift change to lower
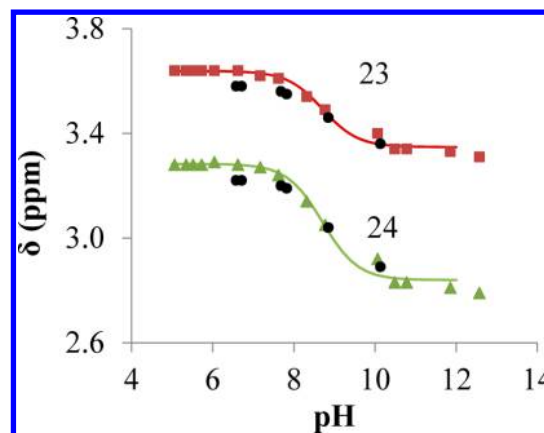

Figure 2. Change of ^{1}H NMR chemical shift of terminal protons 23 and 24 of G5.NH$_2$ as a function of pH. ■ and ▲ symbols stand for G5.NH$_2$ in the absence of AuCl$_x$OH$_y^−$ ions, while ● symbols stand for G5.NH$_2$ in the presence of AuCl$_x$OH$_y^−$ ions.

ppm values (Figure 2) is an indication of higher shielding which may be the result of ion pair formation between the dominant AuCl$_x$OH$_y^−$ anions and the −NH$_3^+$ end groups, resulting in movement of protons from NH$_3^+$ to the direction of AuCl$_x$OH$_y^−$. This observation is in accordance with the one published by Antonietti et al. who observed no classical donor−acceptor complex formation under the circumstances of reduction.[12] It also supports our observation that the AuNPs form in the outer shell of G5.NH$_2$ dendrimer, where the appearance of AuCl$_x$OH$_y^−$ is more probable, in accordance with Figure 1. The presence of Au(III) ions did not change the size of the dendrimer, as we could determine approximately the same diffusion rates for the dendrimer at the corresponding pH as without gold ions published in our previous paper.[25] At high gold ion concentration, the dendrimer assisted reduction of Au(III) was observed.

Cavities in G5.NH$_2$, Cryoporometric Results. Intensive molecular dynamic calculations on PAMAM dendrimers suggest that even in aqueous solutions there may be well defined cavities in the inner sphere of the dendrimer filled with water.[34] These cavities may serve as templates for NPs formation; therefore, a possible reason why we have a higher dendrimer molecule to AuNP ratio than 1:1 in the hybrid particles may be that there is not enough room for gold colloids inside G5.NH$_2$. We believe that collecting further experimental evidence of the existence and features of cavities helps the deeper understanding. Earlier we determined the number of water molecules diffusing with the same rate as G5.NH$_2$, in other words a kind of hydration number, as 3700.[25] In the cryoporometric experiment, step-by-step addition of water to dendrimer may give information if there are preferred places for water; that is, water will first fill these cavities. In Figure 3, we show the results of cryoporometry experiments on dendrimers with different water contents up to 4000 mol of water to 1 mol of G5.NH$_2$.

The cryoporometry experiments show that the added water is confined in cavities in which the melting temperatures of water are around 240 and 252 K when only 1000 water molecules are present. When the number of water molecules is 2000, only that confined water appears where the melting point is around 250 K. When 3000 water molecules for dendrimer are added, this melting point can still be observed but another one close to 273 K appears, indicating the formation of a water layer
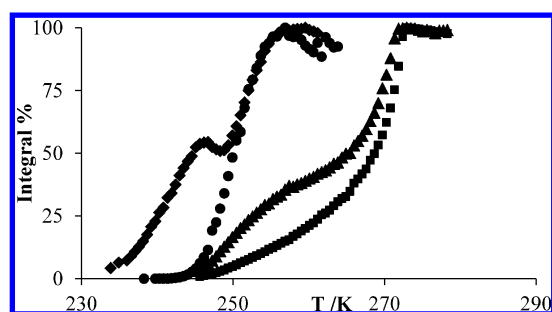
Figure 3. Changes of the integrated intensity of the liquid water peak as a function of temperature. The water dendrimer ratio is (◆) 1000, (●) 2000, (▲) 3000, and (■) 4000.

for which the melting point depression is zero. After adding more water, approximately 4000 per dendrimer, the system loses the coherent structure and starts to flow. If we calculate the pore size in every temperature by eq 2, it results in the cumulative pore size distribution curves. Then, taking the numeric derivatives by the pore size, the differential distribution curve can be given as it is shown in Figure 4.[26,28,35]
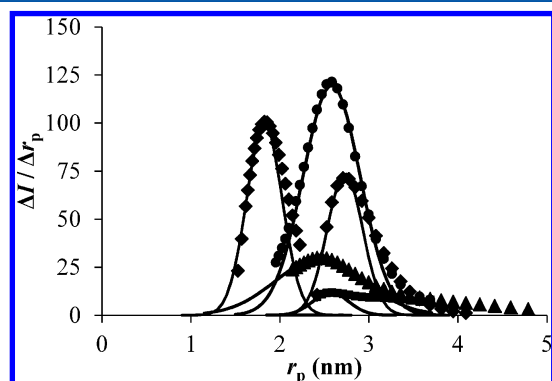
Figure 4. Pore size distribution curves of the swelling G5.NH₂ polymer defined by the radius. The water dendrimer ratio is (◆) 1000, (●) 2000, (▲) 3000, and (■) 4000. Lines represent the Gaussian distribution with the best parameters.

According to curves in Figure 4, two well-determined pore sizes could be detected in the presence of water. When only 1000 water molecules are present, both pores appear with 3.6 and 5.2 nm diameters (1.8 and 2.6 nm radius). When the number of water molecules increases to 2000, only one averaged pore size of 5.4 nm forms. In the presence of 3000 water molecules, this size is still the most probable one but the distribution starts to be broader. In the case of the addition of 4000 water molecules, the distribution is very broad but there is still a weakly defined maximum at around 5.2 nm. At this step, the presence of a continuous water layer is remarkable.

In all ratios, we measured the diffusion rate of the entrapped water molecules at room temperature. In Figure 5, we can see that the diffusion rate of water is slower than that of the free water and independent of the diffusion time. It means that the system is in the restricted diffusion range and that the wall of the pores is penetrable for water, that is, they are connected.[36−38] From the diffusion coefficient, we can calculate the average distance that a water molecule travels by diffusion in the dendrimer gel. In the slowest case when only 1000 water molecules are present, the diffusion coefficient is 1.4×10^{-10} m^2 s^{-1}. The average distance within 1 week, the shortest time
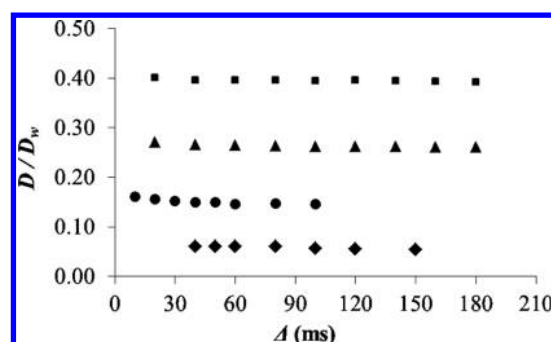

Figure 5. Relative diffusion coefficient of water compared with the free water in the swelled G5.NH₂ dendrimer. The water dendrimer ratio is (◆) 1000, (●) 2000, (▲) 3000, and (■) 4000.

between the mixing and the cryoporometric measurements, is $(\langle x^2 \rangle)^{1/2} = (D \times t)^{1/2} \approx 1$ cm. It means that the mixing of water in the dendrimer was achieved. The reproducibility of the melting curves also proved this (see the Supporting Information, Figure S4); therefore, water diffused within the dendrimer where cavities took place.

The cryoporometric results show that water, even if it is present in a small amount, is in cavities of 3.6 and 5.2−5.6 nm in diameter. These cavities are large compared to the size of the completely hydrated and swelled G5.NH₂ as 6.2 nm.[25,33] The 5.2−5.6 nm pore seems to remain until complete swelling. These cavity sizes can be imagined in the only way that the water droplets exist between dendrimer molecules as Scheme 2

Scheme 2. Possible Picture of the Position of Water Droplets in G5.NH₂ Dendrimers (Upper) and the Encapsulated Gold Nanoparticle Stabilized by 3−4 Dendrimers (Lower)
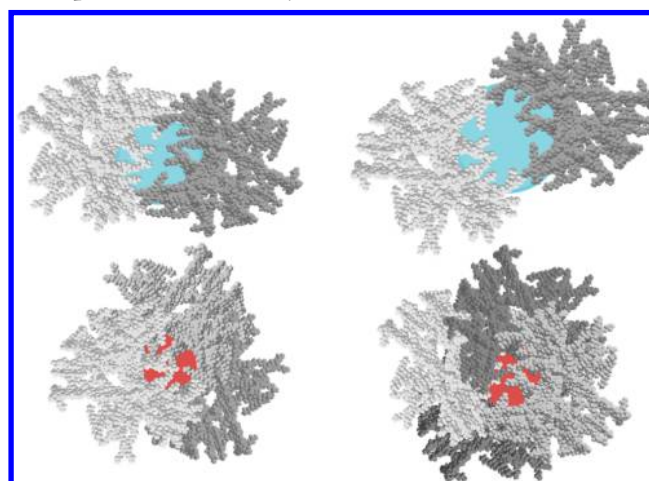
illustrates. After reaching a number of 4000, the characteristic cavities start to disappear, the amount of confined water decreases compared to the layer like water molecules, and a continuous water phase forms around the G5.NH₂ molecules. It does not mean that there are no cavities in G5.NH₂ in solution; it rather means that it is not as characteristic as in the higher generations.

The cryoporometric experiments allow us to draw the following consequences. Under certain circumstances, the G5 PAMAM dendrimers may entrap nanoparticles because there are cavities between 2 or 3 dendrimers. However, we should point out that these results are strictly valid only for G5.NH₂

and water. In other words, the definition of "cavity in dendrimers" may depend on the system under study and the experimental method. As an example, smaller gold atomic assemblies, 1−2 nm, were entrapped successfully into a functionalized G4 dendrimer.[19]

CONCLUSION

The principal result of this work is that we verified the exceptional templating behavior of PAMAM_G5.NH$_2$ in the formation of gold nanoparticles. It is neither the classical 1:1 encapsulation nor the classical steric stabilization by adsorption. Probably 3−4 dendrimer molecules encapsulate the AuNPs, resulting in 8−9 nm large hybrid particles. The conclusion was based on the following results. First, the detailed analysis of diffusion NMR showed that most probably 3−4 dendrimers stabilize one gold nanoparticle of 2−3 nm in diameter. The size of the hybrid particles formed is between 8 and 9 nm similarly to the trimer and tetramer dendrimers. Second, the cryoporometric experiments verified that during hydration there are cavities in PAMAM_G5.NH$_2$ until the complete hydration occurs. The diffusion of water molecules in the swelling PAMAM_G5.NH$_2$ indicates a penetrable structure; no well-defined pore wall is present. Third, high resolution ^{1}H NMR showed that the gold nanoparticles are in the outermost part of G5.NH$_2$ and the interaction with Au(III) ions before the reduction is a weak electrostatic association. As a summary, if 3−4 dendrimer molecules entrap one gold nanoparticle, the size at the beginning may be determined by the ratio of the nucleation and aggregation rates of gold atoms formed by the reduction. In a later phase, the association of gold containing dendrimers leads to the template effect, resulting in dendrimer encapsulated nanoparticles.

ASSOCIATED CONTENT

ⓢ Supporting Information

Results of PGSE NMR spectroscopy, NMR titration, and cryoporometric experiments. This material is available free of charge via the Internet at http://pubs.acs.org.

AUTHOR INFORMATION

Corresponding Author
*E-mail: banyai.istvan@science.unideb.hu.

Author Contributions

The manuscript was written through contributions of all authors. Mónika Kéri has made most of the NMR experiments and evaluations and prepared a large part of the manuscript.

Notes

The authors declare no competing financial interest.

ACKNOWLEDGMENTS

REFERENCES

(1) Shan, Y.; Luo, T.; Peng, C.; Sheng, R.; Cao, A.; Cao, X.; Shen, M.; Guo, R.; Tomas, H.; Shi, X. Gene Delivery Using Dendrimer-Entrapped Gold Nanoparticles as Nonviral Vectors. *Biomaterials* **2012**, *33*, 3025−3035.

(2) Gröhn, F.; Bauer, B. J.; Akpalu, Z. A.; Jackson, C. L.; Amis, E. J. Dendrimer Templates for the Formation of Gold Nanoclusters. *Macromolecules* **2000**, *33*, 6042−6050.

(3) Balogh, L.; Tomalia, D. A. Poly(amidoamine) Dendrimer-Templated Nanocomposites. 1. Synthesis of Zerovalent Copper Nanoclusters. *J. Am. Chem. Soc.* **1998**, *120*, 7355−7356.

(4) Balogh, L.; Valluzzi, R.; Laverdure, K. S.; Gido, S. P.; Hagnauer, G. L.; Tomalia, D. A. Formation of Silver and Gold Dendrimer Nanocomposites. *J. Nanopart. Res.* **1999**, *1*, 353−368.

(5) Crooks, R. M.; Zhao, M. Q.; Sun, L.; Chechik, V.; Yeung, L. K. Dendrimer-Encapsulated Metal Nanoparticles: Synthesis, Characterization, and Applications to Catalysis. *Acc. Chem. Res.* **2001**, *34*, 181−190.

(6) Garcia, M. E.; Baker, L. A.; Crooks, R. M. Preparation and Characterization of Dendrimer-Gold Colloid Nanocomposites. *Anal. Chem.* **1999**, *71*, 256−258.

(7) Zhao, M. Q.; Crooks, R. M. Intradendrimer Exchange of Metal Nanoparticles. *Chem. Mater.* **1999**, *11*, 3379−3385.

(8) Zhao, M. Q.; Crooks, R. M. Dendrimer-Encapsulated Pt Nanoparticles: Synthesis, Characterization, and Applications to Catalysis. *Adv. Mater.* **1999**, *11*, 217−220.

(9) Zhao, M. Q.; Crooks, R. M. Homogeneous Hydrogenation Catalysis with Monodisperse, Dendrimer-Encapsulated Pd and Pt Nanoparticles. *Angew. Chem., Int. Ed.* **1999**, *38*, 364−366.

(10) Myers, V. S.; Weir, M. G.; Carino, E. V.; Yancey, D. F.; Pande, S.; Crooks, R. M. Dendrimer-Encapsulated Nanoparticles: New Synthetic and Characterization Methods and Catalytic Applications. *Chem. Sci.* **2011**, *2*, 1632−1646.

(11) Scott, R. W. J.; Wilson, O. M.; Crooks, R. M. Synthesis, Characterization, and Applications of Dendrimer-Encapsulated Nanoparticles. *J. Phys. Chem. B* **2005**, *109*, 692−704.

(12) Antonietti, M.; Grohn, F.; Hartmann, J.; Bronstein, L. Nonclassical Shapes of Noble-Metal Colloids by Synthesis in Microgel Nanoreactors. *Angew. Chem., Int. Ed.* **1997**, *36*, 2080−2083.

(13) Ye, H. C.; Crooks, R. M. Electrocatalytic O$_2$ Reduction at Glassy Carbon Electrodes Modified with Dendrimer-Encapsulated Pt Nanoparticles. *J. Am. Chem. Soc.* **2005**, *127*, 4930−4934.

(14) Albiter, M. A.; Crooks, R. M.; Zaera, F. Adsorption of Carbon Monoxide on Dendrimer-Encapsulated Platinum Nanoparticles: Liquid versus Gas Phase. *J. Phys. Chem. Lett.* **2010**, *1*, 38−40.

(15) Hu, J. J.; Xu, T. W.; Cheng, Y. Y. NMR Insights into Dendrimer-Based Host Guest Systems. *Chem. Rev.* **2012**, *112*, 3856−3891.

(16) Gomez, M. V.; Guerra, J.; Myers, V. S.; Crooks, R. M.; Velders, A. H. Nanoparticle Size Determination by ^{1}H NMR Spectroscopy. *J. Am. Chem. Soc.* **2009**, *131*, 14634−14635.

(17) Gomez, M. V.; Guerra, J.; Velders, A. H.; Crooks, R. M. NMR Characterization of Fourth-Generation PAMAM Dendrimers in the Presence and Absence of Palladium Dendrimer-Encapsulated Nanoparticles. *J. Am. Chem. Soc.* **2009**, *131*, 341−350.

(18) Wales, C. H.; Berger, J.; Blass, S.; Crooks, R. M.; Asherie, N. Quasi-Elastic Light Scattering of Platinum Dendrimer-Encapsulated Nanoparticles. *Langmuir* **2011**, *27*, 4104−4109.

(19) Kim, Y. G.; Oh, S. K.; Crooks, R. M. Preparation and Characterization of 1−2 nm Dendrimer-Encapsulated Gold Nanoparticles Having Very Narrow Size Distributions. *Chem. Mater.* **2004**, *16*, 167−172.

(20) Ackerson, C. J.; Jadzinsky, P. D.; Sexton, J. Z.; Bushnell, D. A.; Kornberg, R. D. Synthesis and Bioconjugation of 2 and 3 nm-Diameter Gold Nanoparticles. *Bioconjugate Chem.* **2010**, *21*, 214−218.

(21) Lu, Y.; Wang, L. X.; Chen, D. J.; Wang, G. K. Determination of the Concentration and the Average Number of Gold Atoms in a Gold Nanoparticle by Osmotic Pressure. *Langmuir* **2012**, *28*, 9282−9287.

(22) Guo, R.; Wang, H.; Peng, C.; Shen, M.; Pan, M.; Cao, X.; Zhang, G.; Shi, X. X-Ray Attenuation Property of Dendrimer-Entrapped Gold Nanoparticles. *J. Phys. Chem. C.* **2010**, *114*, 50−56.

(23) Shi, X.; Wang, S.; Sun, H.; Baker, J. R. Improved Biocompatibility of Surface Functionalized Dendrimer-entrapped Gold Nanoparticles. *Soft Matter* **2007**, *3*, 71−74.

(24) Wang, H.; Zheng, L.; Guo, R.; Peng, C.; Shen, M.; Shi, X.; Zhang, G. Dendrimer-Entrapped Gold Nanoparticles as Potential CT Contrast Agents for Blood Pool Imaging. *Nanoscale Res. Lett.* **2012**, *7*, 1−8.

(25) Banyai, I.; Keri, M.; Nagy, Z.; Berka, M.; Balogh, L. P. Self-Diffusion of Water and Poly(amidoamine) Dendrimers in Dilute Aqueous Solutions. *Soft Matter* **2013**, *9*, 1645−1655.

(26) Strange, J. H.; Rahman, M.; Smith, E. G. Characterization of Porous Solids by NMR. *Phys. Rev. Lett.* **1993**, *71*, 3589−3591.

(27) Mitchell, J.; Webber, J. B. W.; Strange, J. H. Nuclear Magnetic Resonance Cryoporometry. *Phys. Rep.* **2008**, *461*, 1−36.

(28) Petrov, O. V.; Furo, I. NMR Cryoporometry: Principles, Applications and Potential. *Prog. Nucl. Magn. Reson. Spectrosc.* **2009**, *54*, 97−122.

(29) Ammann, C.; Meier, P.; Merbach, A. E. A Simple Multi-Nuclear NMR Thermometer. *J. Magn. Reson.* **1982**, *46*, 319−321.

(30) Nesmelova, V. I.; Fedotov, V. D. Self-Diffusion and Self-Association of Lysozyme Molecules in Solution. *Biochim. Biophys. Acta, Protein Struct. Mol. Enzymol.* **1998**, *1383*, 311−316.

(31) Ramzi, A.; Scherrenberg, R.; Brackman, J.; Joosten, J.; Mortensen, K. Intermolecular Interactions Between Dendrimer Molecules in Solution Studied by Small-Angle Neutron Scattering. *Macromolecules* **1998**, *31*, 1621−1626.

(32) Lévay, B. Studies on Self-Association Equilibria by Self-Diffusion Measurements. *J. Phys. Chem.* **1973**, *77*, 2118−2121.

(33) van Dongen, M. A.; Orr, B. G.; Holl, M. M. B. Diffusion NMR Study of Generation-Five PAMAM Dendrimer Materials. *J. Phys. Chem. B* **2014**, *118*, 7195−7202.

(34) Maiti, P. K.; Cagin, T.; Lin, S. T.; Goddard, W. A. Effect of Solvent and pH on the Structure of PAMAM Dendrimers. *Macromolecules* **2005**, *38*, 979−991.

(35) Petrov, O.; Furo, I. A Study of Freezing−Melting Hysteresis of Water in Different Porous Materials. Part I: Porous Silica Glasses. *Microporous Mesoporous Mater.* **2011**, *138*, 221−227.

(36) Cho, C. H.; Hong, Y. S.; Kang, K.; Volkov, V. I.; Skirda, V.; Lee, C. Y. J.; Lee, C. H. Water Self-Diffusion in Chlorella Sp. Studied by Pulse Field Gradient NMR. *Magn. Reson. Imaging* **2003**, *21*, 1009−1017.

(37) Latour, L. L.; Svoboda, K.; Mitra, P. P.; Sotak, C. H. Time-Dependent Diffusion of Water in a Biological Model System. *Proc. Natl. Acad. Sci. U. S. A.* **1994**, *91*, 1229−1233.

(38) Valiullin, R.; Skirda, V. Time Dependent Self-Diffusion Coefficient of Molecules in Porous Media. *J. Chem. Phys.* **2001**, *114*, 452−458.